FEMS Yeast Research, 2024, **24**, foae038
DOI: 10.1093/femsyr/foae038
Advance access publication date: 29 November 2024
Research Article

Exploring polyamine metabolism of the yeast-like fungus, *Emergomyces africanus*

Elizaveta Koroleva[1], Barbra Toplis[1], Malcolm Taylor[2], Corné van Deventer[1], Heidi C. Steffen[1], Christiaan van den Heever[1], Nelesh P. Govender[3,4,5,6,7], Sybren de Hoog[8], Alfred Botha[1,*]

[1]Department of Microbiology, University of Stellenbosch, Stellenbosch, 7600, South Africa
[2]Mass Spectrometry Unit, Central Analytical Facility, University of Stellenbosch, Stellenbosch, 7600, South Africa
[3]Centre for Healthcare-Associated Infections, Antimicrobial Resistance and Mycoses, National Institute for Communicable Diseases, a Division of the National Health Laboratory Service, Johannesburg, 2192, South Africa
[4]Faculty of Health Sciences, University of the Witwatersrand, Johannesburg, 2050, South Africa
[5]Institute for Infection and Immunity, St George's University of London, London, SW17 0RE, United Kingdom
[6]MRC Centre for Medical Mycology, University of Exeter, Exeter, EX4 4QD, United Kingdom
[7]Division of Medical Microbiology, University of Cape Town, Cape Town, 7705, South Africa
[8]Medical Microbiology, Radboud University Medical Center, Nijmegen, 6525 GA, The Netherlands
*Corresponding author. Department of Microbiology, University of Stellenbosch, Private Bag X1, Stellenbosch, South Africa. E-mail: abo@sun.ac.za
Editor: [Miguel Teixeira]

Abstract

Emergomyces africanus is a thermally dimorphic pathogen causing severe morbidity and mortality in immunocompromized patients. Its transition to a pathogenic yeast-like phase in the human host is a notable virulence mechanism. Recent studies suggest polyamines as key players in dimorphic switching, yet their precise functions remain enigmatic. This work aimed to explore polyamine metabolism of two clinical strains of *E. africanus* (CBS 136260 and CBS 140360) in mycelial and yeast-like phases. In this first report of the polyamine profile of *E. africanus*, we reveal, using mass spectrometry, spermidine, and spermine as the major polyamines in both phases. The secretion of these amines was significantly higher in the pathogenic yeast-like phase than in the mycelial phase, warranting further investigation into the implications thereof on virulence. Additionally, we detected the activity of several polyamine biosynthesis enzymes, including arginine decarboxylase, agmatinase, arginase, and ornithine decarboxylase, with significant differences in enzyme expression between morphological phases and strains. Finally, we provide initial evidence for the requirement for spermine, spermidine, and putrescine during the thermally induced dimorphic switch of *E. africanus*, with strain-specific differences in the production of these amines. Overall, our study presents novel insight into polyamine metabolism and its role in dimorphism of *E. africanus*.

Keywords: polyamine biosynthesis; dimorphism; ornithine decarboxylase; spermine; *Emergomyces africanus*

Introduction

Emergomyces africanus, formerly *Emmonsia*, is a thermally dimorphic opportunistic pathogen (Dukik et al. 2017). This species has rapidly gained clinical relevance in South Africa, as it causes a severe, and often fatal, systemic infection in immunocompromized patients (Schwartz et al. 2015, Schwartz et al. 2018b, Hoving 2024). In a recent decade-long review of laboratory-confirmed cases of endemic mycoses in South Africa, emergomycosis accounted for 23% (154/682) of cases (Mapengo et al. 2022). However, this is a minimum estimate since ∼30% of the 682 endemic mycoses cases did not have a corresponding culture or molecular identification and were thus unspecified. To date, only a severe disseminated form of *E. africanus* infection has been described in people living with advanced HIV disease in southern Africa and was associated with a high crude mortality (54%).

A notable virulence mechanism of *E. africanus* is its temperature-induced morphological transition from a mycelial phase (26°C) to a yeast-like phase (37°C), which is essential for pathogenesis and dissemination within the host (Boyce and Andrianopoulos 2015, Dukik et al. 2017). The mycelial phase of this fungus is believed to be present in the soil (Schwartz et al. 2018a) with transmission occurring through the inhalation of airborne infectious conidia. This subsequently leads to the onset of emergomycosis in severely immunosuppressed hosts following the temperature-induced switch of the fungus to the yeast-like phase (Reddy et al. 2023). Apart from the identified exposure route and dimorphism, little is known of the pathobiology of *E. africanus*, although studies on other pathogenic fungi suggest that polyamines and the metabolic pathways involved in their biosynthesis, may play a role in dimorphism (Guevara-Olvera et al. 1993, San-Blas et al. 1996, 1997, Kummasook et al. 2013).

Polyamines are low-molecular-weight, biogenic cations that participate in a diverse range of biological processes (Igarashi and Kashiwagi 2019, Schibalski et al. 2024). In fungi, the major polyamines are putrescine, spermidine, and spermine, while the less-commonly reported amines include agmatine and cadaverine (Rocha and Wilson 2019). These molecules are essential for life and are known to play a role in fungal cell growth (Chattopadhyay et al. 2002, Toplis et al. 2021), protein synthesis (Vindu et al. 2021), stress tolerance (Chattopadhyay et al. 2006, Valdés-Santiago et al. 2010), differentiation (Calvo-Mendez et al. 1987, Medina et al. 2022), and virulence (Rocha et al. 2020, Schaefer et al.

Received 17 July 2024; **revised** 4 November 2024; **accepted** 28 November 2024

2020). As insufficient levels of these amines hinder growth (Pfaller et al. 1990, Toplis et al. 2021), and excess amounts can be cytotoxic (Hu and Pegg 1997), the fungal metabolism tightly regulates polyamine levels to maintain homeostasis (Miller-Fleming et al. 2015) via a combination of polyamine transport, catabolism, and biosynthesis.

Polyamines are synthesized from amino acids such as arginine, ornithine, lysine, and methionine via several possible routes (Fig. 1). The synthesis of putrescine (considered the first step in polyamine production) can be achieved via two possible pathways dependent on the presence of ornithine and/or arginine. In most fungi, putrescine is synthesized via ornithine decarboxylase (El-Sayed et al. 2019). The higher polyamines, spermidine, and spermine, are synthesized from putrescine via the sequential addition of aminopropyl groups derived from decarboxylated S-adenosylmethionine by spermidine- and spermine synthase enzymes, respectively (Valdés-Santiago and Ruiz-Herrera 2014). Lastly, the minor polyamine cadaverine is generally considered to be the product of lysine decarboxylation via lysine decarboxylase activity, although some studies suggest the involvement of ornithine decarboxylase in this reaction (Zarb and Walters 1994, Walters and Cowley 1996). In addition to the biosynthetic processes, some polyamines may be converted to form lower polyamines via retroconversion mechanisms (Fig. 1) involving the oxidation of either the acetylated or non-acetylated form of higher polyamines (Miller-Fleming et al. 2015). These mechanisms form a cyclic pattern in polyamine metabolism, facilitating the regulation of their cellular concentrations.

Polyamines, and the metabolic pathways involved in their synthesis, have gained recent attention for their involvement in the onset of various pathologies, including microbial infections (Rollins-Smith et al. 2019, Schaefer et al. 2020, Schibalski et al. 2024). This is unsurprising, given the fundamental importance of polyamines in the biology of living organisms. However, unlike other microbes, research into polyamine metabolism of fungi, particularly that of mammalian pathogens is limited, which complicates our understanding of the function of these molecules in fungal virulence. Thus, the aim of this study was to explore the polyamine biosynthesis pathways of two clinical strains of *E. africanus* and to obtain an indication of the role of polyamines in the dimorphism of the fungus.

Materials and methods

Fungal strains and culture maintenance

All experimental procedures in this study were performed using *E. africanus* clinical strains CBS 136260 and CBS 140360, originally obtained from the culture collection of the National Institute for Communicable Diseases, South Africa. The mycelial phase was maintained (26°C in the dark) via routine subculturing on Brain Heart Infusion (BHI) medium (pH 7.4, Oxoid, Basingstoke, UK), supplemented with 2% bacteriological agar (Merck, Modderfontein, South Africa). The yeast-like cells of *E. africanus* were generated by transferring a mycelial plug onto BHI agar and incubating at 37°C in the dark. After several repeated transfers on BHI agar plates, the yeast growth was transferred to a test tube containing 5 ml BHI broth and incubated in the dark at 37°C on a TC-7 tissue culture roller drum (60 rpm; New Brunswick Scientific Co. Inc., Edison, USA). Unless otherwise specified, the yeast-like phase served as the working culture (maintained by repeated subculturing in BHI broth), and for experiments with the mycelial phase, hyphal growth was initiated from this working culture by inoculating yeast-like cells into BHI broth and incubating at 26°C. Cryocultures of the mycelial phase of *E. africanus* were periodically revived throughout the study to avoid acclimatization or in-lab mutation.

Qualitative screening of polyamine production

The potential for polyamine production was initially tested by screening *E. africanus* for the decarboxylation of the amino acids L-arginine, L-lysine, and L-ornithine on Long Ashton Decarboxylase (LAD) agar medium (pH 5.5) (Cloete et al. 2009), with modifications according to Lerm et al. (2017). The medium was supplemented with either 2 g/l L-arginine monohydrochloride (Sigma-Aldrich, St. Louis, USA), 3.36 g/l L-lysine (Sigma-Aldrich, St. Louis, USA), or 3.2 g/l L-ornithine monohydrochloride (Sigma-Aldrich, St. Louis, USA). The negative control consisted of LAD medium without amino acid supplementation. To screen the mycelial phase of *E. africanus*, 10 µl suspensions of 2-day-old yeast-like cells, cultured on BHI agar at 37°C, were spot inoculated in the centre of the LAD plates. These were incubated in the dark for 5 weeks at 26°C. The yeast-like phase was screened by streaking a large loopful of 2-day-old yeast-like cells, previously cultured on BHI agar, onto the LAD plates. These were incubated in the dark at 37°C for 5 days, with daily monitoring. Pink colouration of the LAD plates was considered a positive reaction, indicative of decarboxylation of the supplemented amino acid and potential polyamine production.

Growth conditions and protein extract preparation for enzyme activity assays

Strains were initially cultured in the yeast-like phase at 37°C for 2 days in 5 ml BHI broth, whereafter cells were counted using a haemocytometer (Improved Neubauer, Marienfeld Superior, Germany) and inoculated into 50 ml liquid BHI broth in a conical flask (500 ml) at a concentration of 1×10^7 cells/ml. The cultures were incubated at either 37°C (yeast-like phase) or 26°C (mycelial phase) on an orbital shaker (Model G53, New Brunswick Scientific Co. Inc., Edison, USA) at 180 rpm and 155 rpm, respectively. Following incubation at the respective conditions, biomass was harvested for enzyme assays during the mid-to-late exponential growth stage of the respective phases, determined via the preliminary construction of growth curves at the same growth conditions (Figs S1 and S2).

Crude protein extracts were prepared as described by Lerm et al. (2017), with some modifications. Briefly, while yeast-like cells were harvested and washed via centrifugation (8000 *g*, 2 min; Heraeus Biofuge 13, Hanau, Germany), mycelial biomass was harvested and washed by filtration through a Whatman #2 filter (Whatman, Maidstone, England). Thereafter, cell lysis was carried out via vigorous mixing with glass beads (425–600 µm; Sigma-Aldrich, St. Louis, USA). The protein in the supernatant from both yeast-like and mycelial phases was quantified using the BioRad protein assay dye reagent (BioRad Laboratories, Hercules, USA) with bovine serum albumin (Roche, Basel, Switzerland) as a standard. The protein extract was used for enzyme assays immediately after quantification.

Arginase assay

A modified version of Shimke's colorimetric method (Corraliza et al. 1994, Toplis et al. 2020), with additional adaptations for the purpose of this study, was used to measure arginase activity. An aliquot of crude protein extract containing 50 µg of protein was added to a reaction mixture to a total volume of 500 µl. The mixture was incubated at 37°C for 30 min. Following

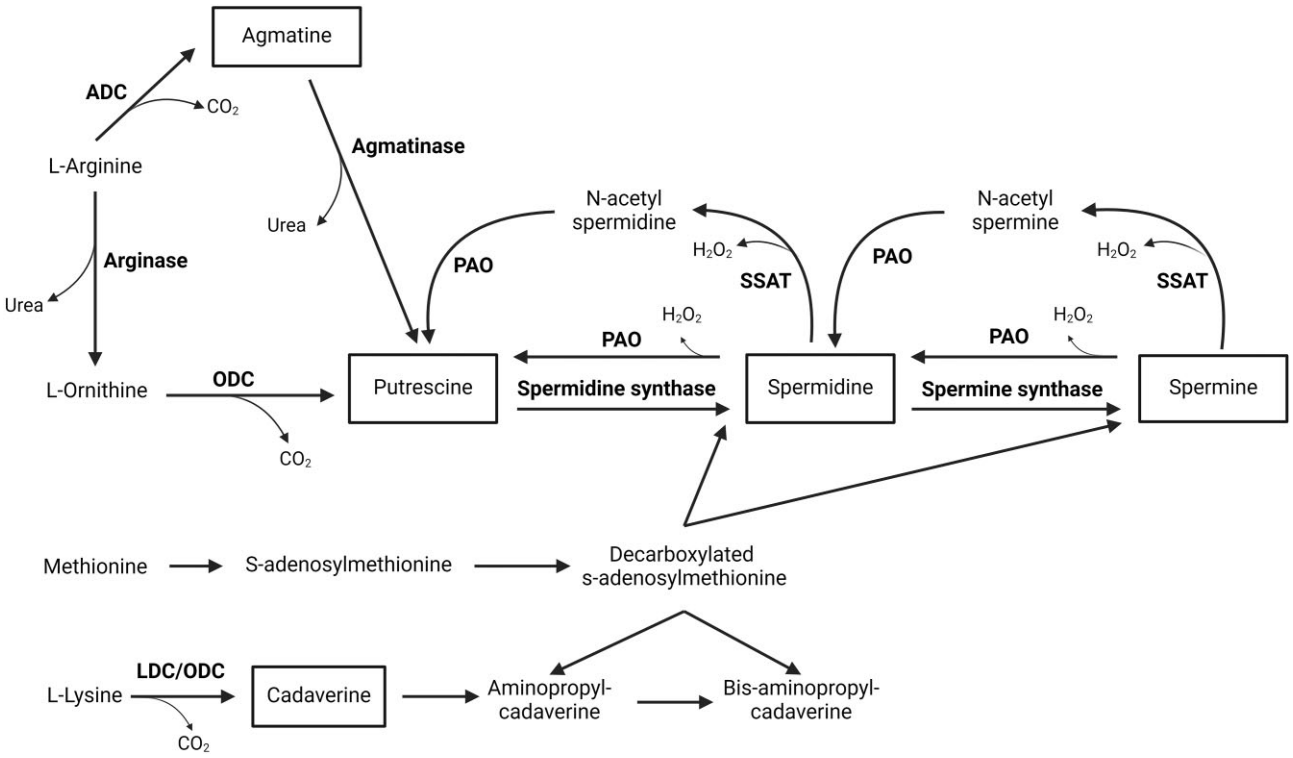

Figure 1. Summary of proposed polyamine biosynthesis pathways in fungi. ADC, arginine decarboxylase; ODC, ornithine decarboxylase; LDC, lysine decarboxylase; PAO, polyamine oxidase; and SSAT, spermidine/spermine N-acetyl transferase. Compiled from: Walters and Cowley (1996), Miller-Fleming et al. (2015), and Rocha and Wilson (2019). (Created with BioRender.com).

the colour development of the stopped reaction using a 9% α-isonitrosopropiophenone (Sigma-Aldrich, St. Louis, USA) solution (prepared in 95% ethanol), the absorbance was measured at 540 nm with a microplate reader (iMark™ Microplate Absorbance Reader, BioRad, California, USA) using 200 µl aliquots dispensed in a 96-well plate (Greiner Bio-one, Kremsmuster, Austria). A reaction mixture without substrate served as a blank for the absorbance readings and an additional reaction mixture without protein was included as a negative control. A calibration curve constructed with increasing urea (Sigma-Aldrich, St. Louis, USA) concentrations was used to calculate the quantity of urea produced.

Agmatinase assay

Agmatinase activity was determined using a method adapted from Iyer et al. (2002) and Toplis et al. (2020), with modifications. An aliquot of protein extract containing 400 µg protein was added to a reaction mixture (total volume 200 µl) consisting of 50 mM Tris-HCl (pH 8.0), 2 mM $MnCl_2$, and 10 mM acetohydroxamic acid (Sigma-Aldrich, St. Louis, USA). Following the colour development of the stopped reaction using 15 µl of a 9% α-isonitrosopropiophenone solution (prepared in 95% ethanol), the absorbance at 540 nm of 200 µl reaction mixture aliquots was measured in a 96-well plate. A reaction mixture without substrate served as a blank for the absorbance readings and a reaction mixture without protein was included as a negative control. A calibration curve constructed with increasing amounts of urea was used to quantify urea production.

Ornithine decarboxylase assay

Ornithine decarboxylase activity was determined based on the methods described by Luqman et al. (2013), relying on the detection of putrescine produced from L-ornithine. One hundred microlitres of crude protein extract were transferred to a microcentrifuge tube containing 400 µl reaction mixture consisting of 2.5 mM β-mercaptoethanol (Riedel-de Haën, Seelze, Germany), 1.5 mM EDTA (Merck, Modderfontein, South Africa), 75 nM pyridoxal-5-phosphate (Sigma-Aldrich, St. Louis, USA), and 3 mM L-ornithine monohydrochloride in 150 mM phosphate buffer (pH 7.1). The reaction was terminated after 30 min of incubation at 37°C by adding 400 µl 1 M perchloric acid (Saarchem, Krugersdorp, South Africa), and the precipitate was removed via centrifugation (5000 *g*, 5 min). Following the separation of the putrescine-containing fraction, 200 µl 10 mM trinitrobenzenesulfonic acid (Sigma-Aldrich, St. Louis, USA), prepared in 1-pentanol (Sigma-Aldrich, St. Louis, USA), was then added to the organic phase, whereafter the sample was thoroughly mixed for 1 min on a vortex, before adding 400 µl dimethyl sulfoxide (DMSO) (Calbiochem, Billerica, USA) and additional mixing for 1 min. Following centrifugation (3000 *g*; 5 min), the absorbance of the upper layer was measured at 415 nm in the microplate reader using 200 µl aliquots in a 96-well plate. A reaction without L-ornithine served as a blank for the absorbance readings and a reaction without protein extract served as a negative control. Putrescine was quantified based on a calibration curve prepared with putrescine (25–500 µM; Sigma-Aldrich, St. Louis, USA) diluted in phosphate buffer (0.1 M; pH 7.0).

Fungal polyamine analysis

Chemicals

The polyamine standards agmatine sulphate (≥97%), spermidine trihydrochloride (≥99%), spermine (≥96%), and cadaverine dihydrochloride (98%), as well as the internal standard heptylamine (99%), were obtained from Sigma-Aldrich (St. Louis,

USA). Putrescine dihydrochloride (≥98%) was obtained from Toronto Research Chemicals (Toronto, Canada). Acetonitrile (High-performance liquid chromatography-grade) was purchased from Sigma-Aldrich (St. Louis, USA). Ultrapure water was prepared by a Milli-Q water purification system (Millipore, Bedford, USA) and was used for the preparation of all buffers and reagents.

Preparation of standard solutions

Individual standard stock solutions of each polyamine (10 mM) were prepared in 0.1 M HCl and stored at −20°C in the dark until analysis. A series of mixed standard solutions of five polyamines (agmatine, cadaverine, putrescine, spermidine, and spermine) were prepared by mixing each stock solution in protein-precipitated growth media. Standard mixtures were prepared just before derivatization to avoid degradation.

Growth conditions for polyamine analysis of growth and dimorphic switching

For the detection of intracellular and extracellular polyamines, mycelial and yeast-like phases of *E. africanus* were initially cultured in BHI broth on an orbital shaker for 48 h at 26°C (155 rpm) and on a tissue culture roller drum at 37°C (60 rpm), respectively. Mycelial biomass was harvested via filtration through a Whatman #2 filter and washed twice with physiological saline solution (PSS, 0.89% NaCl). Yeast-like cells were harvested via centrifugation (10 000 *g*; 2 min), washed twice in PSS, and counted using a haemocytometer.

A polyamine-free medium (PFM) (pH 5.5 ± 0.2) consisting of 0.67% yeast nitrogen base (Difco, Becton, Dickinson and Company, USA), 2% glucose, 0.2% L-arginine monohydrochloride, 0.32% L-ornithine monohydrochloride, and 0.278% L-lysine was formulated to ensure the availability of amino acid substrates for polyamine biosynthesis according to the known metabolic pathways. It also served as the minimal medium for the rest of the study. The PFM was subsequently inoculated with a concentration of either 1×10^7 yeast-like cells/ml or 0.1 g fresh weight mycelial biomass (equivalent to ca. 0.13 g/l dry weight) and incubated in the dark at 37°C and at 26°C on an orbital shaker at 180 and 155 rpm, respectively for 2 days.

For the measurement of intracellular polyamine levels during dimorphic switching, 0.1 g fresh weight mycelial biomass (initiated from a 1 mm × 1 mm mycelial plug of *E. africanus*) was inoculated into PFM and incubated at 37°C on an orbital shaker at 180 rpm for 10 days. Polyamine levels were measured at 24-h intervals during the switching process.

All experiments were performed in 25 ml liquid cultures in 250 ml conical flasks using biological triplicates.

Sample preparation

Following incubation in PFM, cell-free supernatants for the detection of extracellular polyamines in the yeast-like phase were prepared by harvesting 1 ml of the culture medium, centrifuging at 10 000 *g* for 2 min and transferring the cell-free supernatant to a clean microcentrifuge tube. For mycelial growth, as well as biomass during the dimorphic switch, the culture medium was filtered through a cellulose nitrate filter (0.45 µm; Sartorius, Goettingen, Germany) and 1 ml of the filtrate was transferred to a clean microcentrifuge tube.

For the detection of intracellular polyamines, cultures were harvested on a cellulose nitrate filter and washed three times with dH_2O. After the final wash step, the harvested biomass was re-suspended in 500 µl dH_2O and transferred to a 2 ml screw-cap microcentrifuge tube containing an equal volume (ca. 0.5 ml) of acid-washed glass beads (425–600 µm). Following cell lysis via vigorous mixing on a vortex for 15 min, the cells were cooled on ice for 5 min. Cellular debris was pelleted via centrifugation (12 000 *g*; 5 min at 4°C). Perchloric acid was added to a final concentration of 6% v/v. Protein content of the cellular extract was quantified using the BioRad protein assay dye reagent.

Protein precipitation

To remove proteins from the samples prior to analysis, 200 µl of ice cold 1:1 v/v mixture of acetonitrile and 10% trifluoroacetic acid (>99%; Sigma-Aldrich, St. Louis, USA) were added to 100 µl of sample. Following a 10 min incubation at 4°C, samples were centrifuged (13 000 *g*; 5 min) and 50 µl 2.5 M NaOH was added to 200 µl supernatant.

Dansyl derivatisation

Dansyl derivatization of polyamines was performed according to methods described by Liu et al. (2018) and Preti et al. (2015) with modifications. Briefly, 100 µl sample was mixed with 300 µl $NaHCO_3$ (20 g/l) and 500 µl dansyl chloride (DnsCl; 5 g/l in acetonitrile), mixed on a vortex for 30 s and subsequently incubated in the dark at 45°C for 60 min. Following incubation, 100 µl NH_4OH (32% w/v) was added to the mixture to remove excess DnsCl.

Ultraperformance liquid chromatography tandem mass spectrometry analysis

The detection and quantification of intracellular and extracellular polyamines were conducted using ultraperformance liquid chromatography tandem mass spectrometry (UPLC-MS/MS) at the Central Analytical Facility (Mass Spectrometry Unit) at Stellenbosch University, South Africa. Derivatized samples (2 µl) were injected into a Waters Acquity Ultraperformance LC system coupled to a Xevo TQ-MS triple quadrupole mass spectrometer (Waters Corporation, Milford, MA, USA). Separation was carried out on a hydrophobic interaction matrix using an Acquity UPLC BEH C18 (2.1 mm × 100 mm, 1.7 µm) column at 50°C, at a flow rate of 0.4 ml/min. A linear gradient was used for the separation of polyamines over 11 min (Table 1). Solvent A consisted of 0.1% v/v formic acid in Milli-Q water and solvent B consisted of 0.1% v/v formic acid in acetonitrile.

Following separation, samples were subjected to mass spectrometry analysis on a Xevo TQ-MS triple quadrupole mass spectrometer with an electrospray ionization source in positive mode (ESI+). The following conditions were implemented for the analysis: capillary voltage at 3.70 kV, source temperature of 150°C, desolvation temperature of 450°C, cone gas flow rate of 150 l/h, desolvation gas flow rate of 900 l/h, and collision gas (argon) flow rate of 0.19 ml/min. Cone voltages and collision energies for each multiple reaction monitoring (MRM) transition were optimized for each

Table 1. Ultra-performance liquid chromatography solvent gradient conditions for the separation of polyamines.

Time (min)	Solvent A[1] (%)	Solvent B[2] (%)
0	90.0	10.0
0.50	90.0	10.0
8.00	0.0	100.0
9.00	0.0	100.0
9.50	90.0	10.0
11.00	90.0	10.0

[1]Solvent A: 0.1% formic acid in water.
[2]Solvent B: 0.1% formic acid in acetonitrile.

Table 2. Multiple reaction monitoring transitions, cone voltages, and transition energies for the screened polyamines and internal standard (heptylamine).

Analyte	Parent (*m/z*)	Daughter (*m/z*)	Cone (V)	Collision (V)
Putrescine	555.00	170.00	30.0	30.0
		220.00	30.0	25.0
Cadaverine	569.00	170.00	30.0	35.0
		186.30	30.0	30.0
Agmatine	364.00	347.10	15.0	20.0
		170.10	15.0	15.0
Spermidine	845.00	170.00	30.0	35.0
	612.00	170.00	35.0	35.0
Spermine	1135.00	360.00	15.0	45.0
		170.00	15.0	45.0
Heptylamine	349.00	157.00	15.0	40.0
		170.00	15.0	45.0

compound (Table 2). Heptylamine served as the internal standard at a concentration of 10 ppb. Representative MRM chromatograms of the analytes are shown in Fig. S3. Method accuracy, linearity, and limits of detection and quantification were determined in PFM and are shown in Table S1. Instrument control and data acquisition were performed with MassLynx software version 4.2 (Waters Corporation, Milford, MA, USA; https://www.waters.com), and data were processed in TargetLynx XS software (within MassLynx).

Effect of polyamine synthesis inhibitors cyclohexylamine and difluoromethylornithine on dimorphic switching

Cyclohexylamine (CHA) and difluoromethylornithine (DFMO) inhibit the function of spermidine synthase and ornithine decarboxylase enzymes, respectively (Pfaller et al. 1990). In this study, these inhibitors were used to assess their effect on the dimorphic switch of *E. africanus*. To obtain mycelial biomass for this experiment, a 1 mm × 1 mm mycelial plug of *E. africanus* was used to inoculate 50 ml BHI broth in 500 ml conical flasks. These were incubated at 26°C on an orbital shaker at 155 rpm in the dark and routinely subcultured to obtain sufficient growth. Two-day-old cultures served as the inoculum.

Mycelial biomass was harvested via filtration through a sterile Whatman #2 filter and washed twice with PSS. The washed mycelia, ca. 0.1 g in wet weight (ca. 0.13 g/l dry weight), were inoculated into 25 ml PFM (in a 250 ml conical flask) supplemented with either 8 mM CHA or 8 mM DFMO. To investigate the reversal of inhibition, 0.1 mM spermidine and 0.1 mM putrescine were added to the medium containing the inhibitors CHA and DFMO, respectively. Inhibitor-free PFM served as the control.

Flasks were incubated on an orbital shaker at 180 rpm at 37°C for 10 days. Following incubation, the entire culture medium was filtered through a pre-weighed Pasteur pipette containing glass wool to separate hyphal growth and dried at 80°C prior to obtaining a measurement of mycelial biomass (g/ml). Yeast-like cells in the filtrate were counted using a haemocytometer (cells/ml). The extent of the morphological transition was expressed as the number of yeast cells per gram of mycelial biomass (Zhang et al. 2019).

Statistical analysis

All experiments were performed using biological triplicates and quantitative results were statistically analysed using XLSTAT software (Version 2020.4.1, Addinsoft, New York, USA; https://www.xlstat.com). Homogeneity of sample variances and the normality of data were tested using Levene's and Shapiro–Wilk tests, respectively. Normally distributed data with equal variances were analysed for significant differences using either a one-way or two-way analysis of variance (ANOVA). Pairwise comparisons of the means were performed using Fisher's least significant difference (LSD) *post-hoc* test. When values did not conform to ANOVA assumptions of normality and homoscedasticity, data were log-transformed. Pearson's correlation coefficient was used to test for relationships between intracellular polyamine levels and the dimorphic switching process as a function of time and the number of yeast-like cells formed. Significance was determined at $P < .05$.

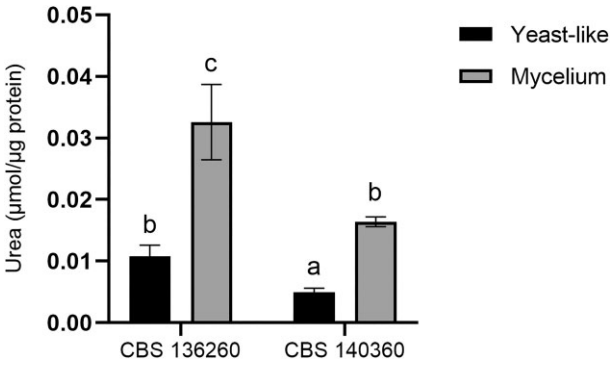

Figure 2. Arginase activity of *E. africanus* CBS 136260 and CBS 140360 in yeast-like (37°C) and mycelial (26°C) phases. Activity is expressed as μmol urea produced per µg crude protein extract after 30 min of incubation. Bars represent the average of three biological replicates and error bars indicate ± standard error of the mean. Means with different letters are indicative of a significant difference ($P < .05$).

Results

Qualitative screening of polyamine production

Both strains of *E. africanus* tested positive for decarboxylase activity, and thus potential polyamine synthesis, in the presence of the amino acids L-arginine and L-ornithine, with a notably weaker reaction in the presence of L-ornithine. This was observed for both mycelial (26°C) and yeast-like (37°C) phases. No apparent L-lysine decarboxylase activity was detected in either strain.

Arginase activity

Arginase enzyme activity was detected in both morphological phases of both strains (Fig. 2). Activity levels were found to be significantly ($P < .05$) higher in CBS 136260 than in the respective

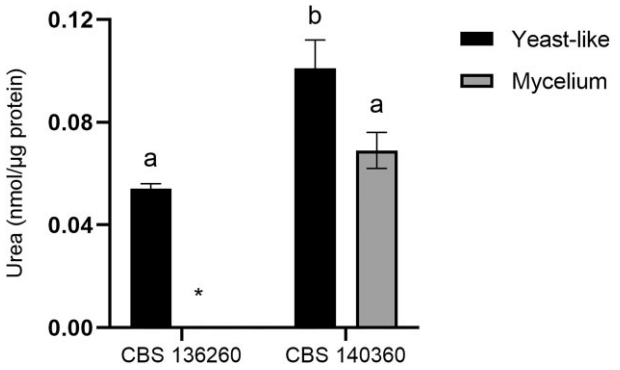

Figure 3. Agmatinase activity of *E. africanus* CBS 136260 and CBS 140360 in yeast-like (37°C) and mycelial (26°C) phases. Activity is expressed as nmol urea produced per µg protein from agmatine sulphate after 1 h incubation. Bars represent the average of three biological replicates and error bars represent ± standard error of the mean. Means with different letters are indicative of a significant difference ($P < .05$). *Below detection limit.

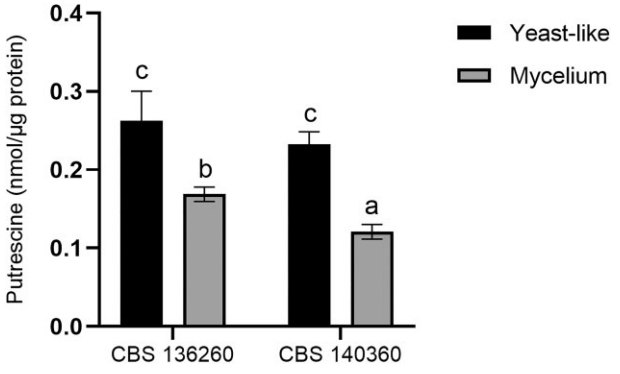

Figure 4. Ornithine decarboxylase activity of *E. africanus* CBS 136260 and CBS 140360 in yeast-like (37°C) and mycelial (26°C) phases. Activity is expressed as nmol putrescine produced per µg crude protein from L-ornithine after 30 min incubation. Bars represent the average of three biological replicates and error bars represent ± standard error of the mean. Means with different letters are indicative of a significant difference ($P < .05$).

phases of CBS 140360. Strikingly, in both strains, arginase activity was found to be over three times higher in the mycelial phase (26°C) than in the yeast-like (37°C) phase.

Agmatinase activity

Both strains of *E. africanus* exhibited agmatinase activity in the yeast-like phase (37°C); however, detectable levels of activity in the mycelial phase (26°C) were only measured in CBS 140360 (Fig. 3). Agmatinase activity in the yeast-like phase of CBS 140360 was significantly ($P < .05$) higher than in the mycelial phase of this strain, as well as the yeast-like phase of CBS 136260.

Ornithine decarboxylase activity

Ornithine decarboxylase activity was detected in both strains at both phases (Fig. 4). Enzyme activity levels were higher in the yeast-like phase (37°C) than the mycelial phase (26°C) in both strains. However, strain CBS 136260 demonstrated significantly ($P < .05$) higher levels of activity than CBS 140360 in the mycelial phase.

Polyamines in growth

Spermidine and spermine were found to be the major polyamines in both strains and morphological phases during vegetative growth (Table 3). Two-way ANOVA of individual polyamines as a function of morphological phase and strain showed significantly higher levels of extracellular spermidine and spermine production in the yeast-like phase than in the mycelial phase. In contrast, intracellular levels of both polyamines were significantly higher in the mycelial phase than the yeast-like phase of CBS 136260; whereas significantly higher intracellular levels of spermine were observed in the yeast-like phase of CBS 140360. Notably, intracellular spermine was produced at comparatively higher levels than spermidine in both strains and phases. In all cases, putrescine and agmatine were found to be minor polyamines and cadaverine levels were below detection limit. No significant differences were observed in putrescine levels across strain or phase. Additionally, comparatively low levels of agmatine were detected intracellularly in yeast-like and mycelial phase supernatants of both strains.

Polyamines in dimorphic switching

Spermidine, spermine, and putrescine were the only detected polyamines during dimorphic switching (Fig. 5). Agmatine and cadaverine levels were below detection limit. Spermidine and spermine were found to be the most abundant ($P < .0001$) throughout the switching process. While putrescine levels gradually increased over time in both strains, the fluctuation of intracellular spermidine and spermine appeared to differ between the two strains during the switching progression (Fig. 5). In CBS 136260, spermidine and spermine showed an initial decline after 48 h followed by an increase during later stages (168–216 h) of the switching process, reaching levels similar to those of the initial stages (Fig. 5A). In contrast, in CBS 140360 these amines appeared to gradually accumulate over time, with a decrease from 192 h (Fig. 5B). These observations were confirmed by Pearson's correlation analysis which indicated a significant moderate correlation between the detected polyamines and the formation of yeast-like cells in CBS 136260 (Table 4). In CBS 140360, polyamines correlated with time after temperature shift in addition to yeast-like cell formation. Furthermore, spermidine levels had a strong positive correlation with spermine and putrescine in both strains, as could be expected based on the polyamine biosynthetic pathways. However, spermine and putrescine levels only significantly correlated in CBS 136260 (Table 4).

Effect of polyamine synthesis inhibitors on dimorphic switching

The dimorphic transition of CBS 136260 was completely inhibited in the presence of 8 mM CHA, but no significant change was observed in the presence of 8 mM DFMO (Fig. 6). In contrast, the transition of CBS 140360 was more strongly inhibited by DFMO compared to CHA, although a significant reduction in switching was observed in the presence of both inhibitors. The addition of 0.1 mM spermidine together with CHA not only reversed the inhibitory effects but also potentiated the morphological transition, improving the switching extent of both CBS 136260 and CBS 140360 compared to controls (Fig. 6). Supplementation with putrescine also had a significant effect on both strains: partial alleviation of DFMO-mediated inhibition was observed for CBS 140360 and the switching extent of CBS 136260 was significantly improved compared to DFMO-exposed CBS 136260 (Fig. 6). However, the latter improvement was not significantly different from the control.

Table 3. Intracellular and extracellular polyamine production of *E. africanus* CBS 136260 and CBS 140360 in yeast-like (37°C) and mycelial (26°C) phases.

	Morphological phase	Strain	Polyamine				
			Agmatine	Cadaverine	Putrescine	Spermidine	Spermine
Intracellular (µg/g protein)	**Yeast-like**	**CBS 136260**	2.20 ± 1.11^{a}	BDL	0.66 ± 0.07^{a}	10.47 ± 1.34^{a}	44.73 ± 10.80^{a}
		CBS 140360	0.99 ± 0.11^{a}	BDL	0.37 ± 0.37^{a}	34.06 ± 10.17^{bc}	286.83 ± 77.94^{c}
	Mycelial	**CBS 136260**	BDL	BDL	1.91 ± 0.59^{a}	49.12 ± 6.96^{c}	181.85 ± 40.94^{bc}
		CBS 140360	BDL	BDL	1.06 ± 0.76^{a}	34.10 ± 8.76^{bc}	127.89 ± 8.63^{b}
Extracellular (µg/g dry weight)	**Yeast-like**	**CBS 136260**	BDL	BDL	3.73 ± 2.62$^{a'}$	1014.43 ± 55.46$^{c'}$	788.52 ± 45.73$^{b'}$
		CBS 140360	BDL	BDL	12.75 ± 7.09$^{a'}$	1010.34 ± 160.45$^{c'}$	1109.81 ± 263.14$^{bc'}$
	Mycelial	**CBS 136260**	2.17 ± 0.54$^{a'}$	BDL	5.96 ± 19.5$^{a'}$	195.00 ± 22.83$^{b'}$	105.63 ± 9.05$^{a'}$
		CBS 140360	0.60 ± 0.60$^{b'}$	BDL	BDL	85.46 ± 21.06$^{a'}$	90.28 ± 21.69$^{a'}$

Results are expressed as the mean of three biological replicates ± standard error of the mean. The production of individual polyamines across different strains and morphological phases was compared using a two-way ANOVA. Different superscript letters indicate statistical significance ($P < .05$). Extra- and intracellular data were analysed separately, therefore only letters of the same prime within the same column are comparable. BDL, below detection limit.

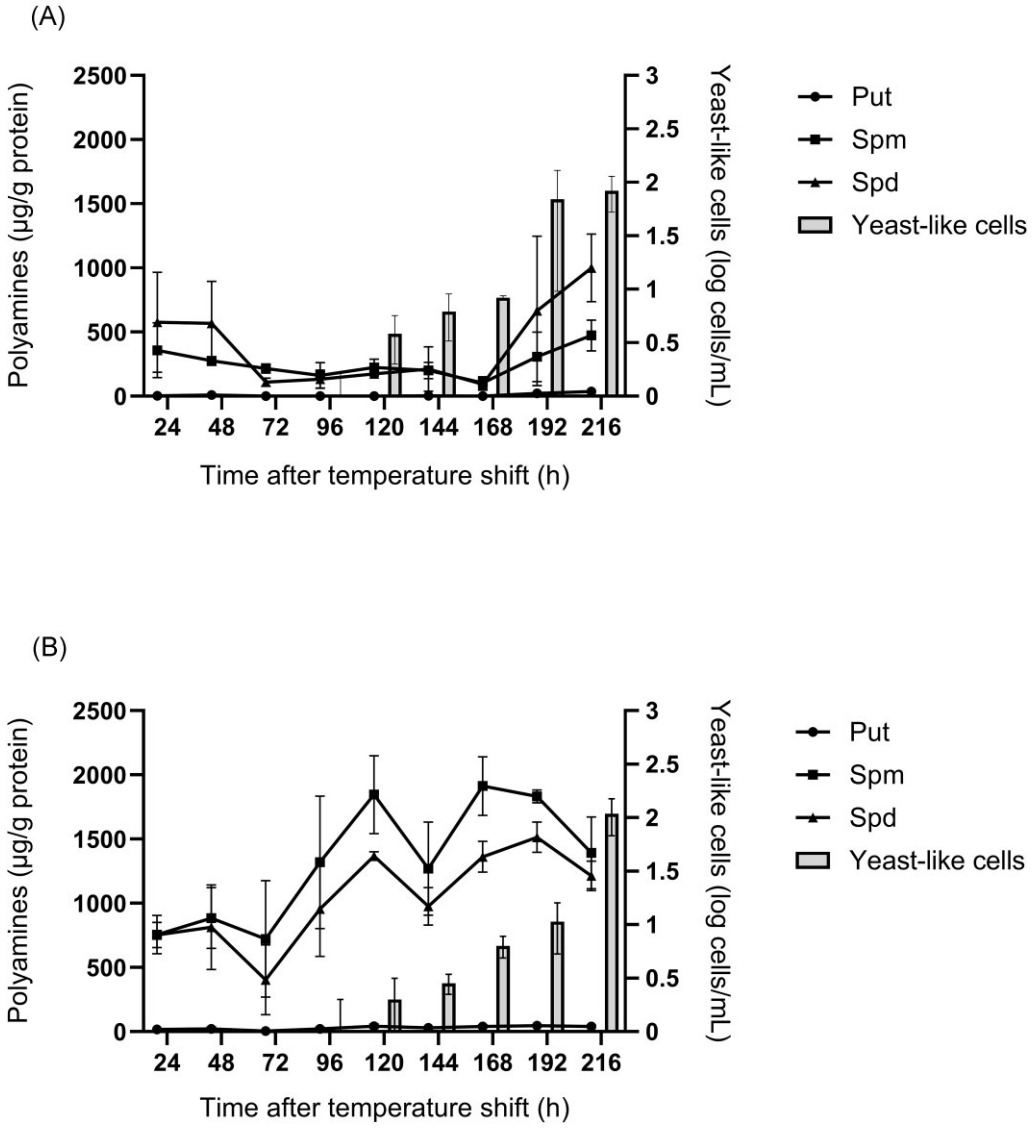

Figure 5. Changes in intracellular polyamine levels during the dimorphic transition of *E. africanus* CBS 136260 (A) and CBS 140360 (B). Polyamine levels are expressed as µg polyamine per g total intracellular protein. Data represent the average of three biological replicates ± standard error of the mean. Put, putrescine; Spm, spermine; and Spd, spermidine.

Table 4. Correlations between intracellular polyamine levels and dimorphic switching progression in *E. africanus* strains CBS 136260 and CBS 140360.

CBS 136260	Time after temperature shift	Putrescine	Spermine	Spermidine
Time after temperature shift				
Putrescine	0.420			
Spermine		0.688		
Spermidine		0.877	0.878	
Yeast-like cells	0.861	0.698	0.450	0.520
CBS 140360				
Time after temperature shift				
Putrescine	0.533			
Spermine	0.527			
Spermidine	0.567	0.789	0.758	
Yeast-like cells	0.868	0.543	0.388	0.505

Pearson correlation coefficients are provided for each variable ($P < .05$). Only statistically significant values are shown.

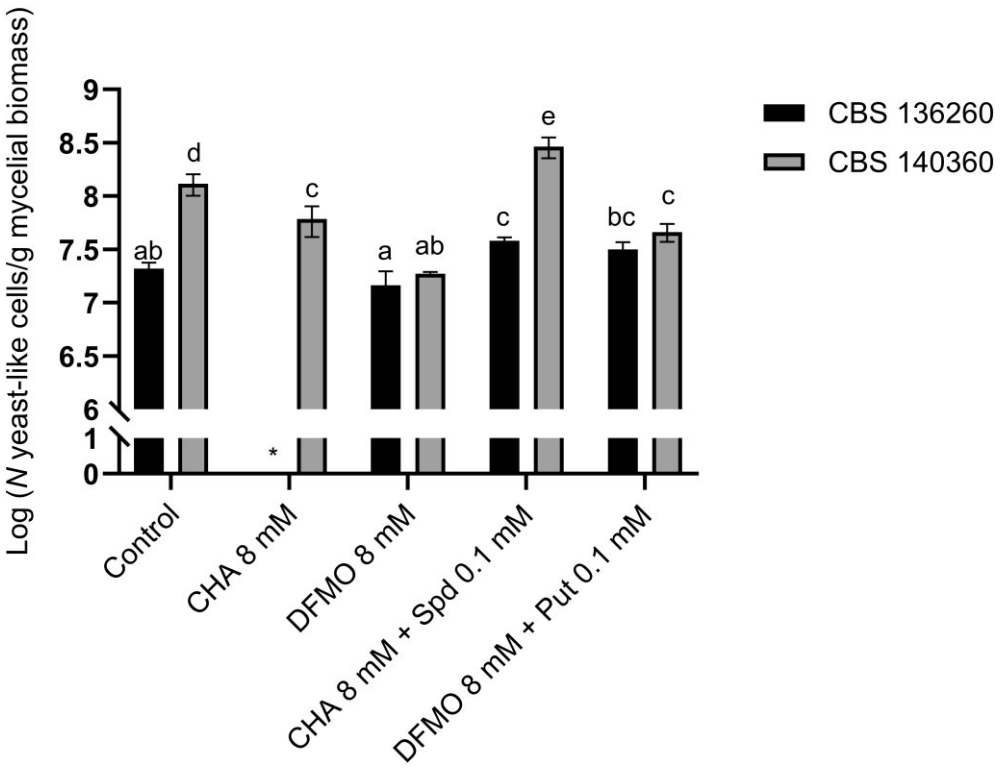

Figure 6. Effect of polyamine biosynthesis inhibitors DFMO and CHA on the thermally induced dimorphic transition of *E. africanus*. The switching extent was quantified after 10 days of incubation at 37°C and expressed as log of the number of yeast-like cells formed per g mycelial dry weight. Bars represent the mean of three biological replicates and error bars indicate the ± standard error of the mean. Statistically significant differences are indicated by different letters ($P < .05$). Put, putrescine and Spd, spermidine. *No yeast-like cells detected.

Overall, CBS 140360 responded more strongly to both inhibitors and supplemented polyamines compared to CBS 136260 (Fig. 6).

Discussion

Polyamines are an important class of metabolites involved in a wide variety of fundamental biological processes (Rocha and Wilson 2019), thus the characterization of their role and metabolism in fungi is key to a deeper understanding of fungal physiology and virulence. In the current study, we provide insights into the role of polyamine metabolism in the dimorphism of *E. africanus*.

The expression of polyamine synthesizing enzymes differed significantly between the morphological phases of *E. africanus*. While arginase appeared to be upregulated during hyphal growth (Fig. 2), agmatinase and ornithine decarboxylase expression were higher in the pathogenic yeast-like phase (Figs 3 and 4)—as was also observed for the closely related dimorphic pathogen *Paracoccidioides brasiliensis* (San-Blas et al. 1996). Ornithine decarboxylase is required for cell budding and could therefore justify the increased expression of this enzyme during the yeast-like phase (San-Blas et al. 1996). Together with the elevated expression of agmatinase in the yeast-like

phase, these results point to a higher demand for putrescine synthesis.

Interestingly, both potential pathways for the synthesis of putrescine from amino acids—via the activities of arginine decarboxylase and agmatinase, as well as via the activities of arginase and ornithine decarboxylase (Fig. 1)—seem to exist in *E. africanus* (Figs 2, 3, and 4). But, in addition to differences in morphological phases, enzyme activity appeared to differ between strains, suggesting intraspecific differences regarding the dominant pathways for polyamine synthesis.

The enzyme activities we recorded corresponded to the polyamine profiles detected with UPLC-MS/MS (Table 3). The seemingly contradictory presence of agmatinase and ornithine decarboxylase activities together with low intracellular levels of putrescine and agmatine (the respective products) suggest that these amines are rapidly channelled into the production of spermidine, and downstream spermine—both of which are major polyamines in *E. africanus*. In accordance with our findings, while spermidine is often a major polyamine (Kummasook et al. 2013, Toplis et al. 2021), spermine is not ubiquitous in all fungal species and is more commonly found in yeasts and dimorphic fungi (Nickerson et al. 1977, Marshall et al. 1979, Cogo et al. 2018). The high intracellular abundance of spermidine and spermine suggests an important role in *E. africanus* cellular functions, such as protein translation (Han et al. 2022), abiotic stress tolerance (Tang et al. 2021), and oxidative stress regulation (Chattopadhyay et al. 2006).

Extracellularly, spermidine and spermine were also present in the highest abundance, with approximately six times more polyamines secreted in the yeast-like phase than in the mycelial phase (Table 3). These are important findings, as the secretion of these polyamines has been reported to disrupt host immune response activation (Lasbury et al. 2007, Rollins-Smith et al. 2019)—significantly contributing to pathogenesis. For instance, animal models of *Pneumocystis* infection suggest that fungal polyamines accumulate in the lungs during infection and lead to reactive oxygen species-mediated apoptosis of alveolar macrophages, an early line of immune defence to inhaled pathogens (Lasbury et al. 2007). In another study, the secretion of spermidine by the amphibian pathogen *Batrachochytrium dendrobatidis* was found to inhibit host lymphocyte proliferation—an important regulator of the immune response (Rollins-Smith et al. 2019). Considering that significantly more polyamines are secreted during the pathogenic growth stage (yeast-like) of *E. africanus* than its non-pathogenic stage (mycelial), it is paramount that the effects of fungal polyamine production on host polyamine levels should be considered in future investigations of fungal virulence and infection progression.

Spermine, spermidine, and putrescine appeared to be significantly correlated with the formation of yeast-like cells, suggesting an association between intracellular polyamine levels and dimorphic switching (Table 4), previously documented in other fungi (San-Blas et al. 1997, Kummasook et al. 2013, Medina et al. 2022). While changes in putrescine levels did not mirror that of spermidine and spermine, as might be expected based on the biosynthesis pathways, putrescine was significantly correlated to spermidine (Fig. 5). Thus, its accumulation over time may be explained by a reduced requirement for its conversion to spermidine. In both strains, increasing levels of spermidine and spermine were associated with the formation of yeast-like cells, supported by similar findings in other species of fungi (San-Blas et al. 1997, Kummasook et al. 2013). Fungal strains in this study were found to differ with regards to polyamine production over time. Strain CBS 140360 showed an increase in spermidine and spermine levels during the early stages of yeast-like cell formation (Fig. 5B), whereas CBS 136260 accumulated spermidine and spermine during later stages of the transition when yeast-like cells were already detectable in the culture medium (Fig. 5A). This points to potential intraspecies variation, and further study into the expression of polyamine synthesizing genes, and at smaller time intervals during the transition, could shed light onto the observed differences.

To confirm the requirement for polyamines during the dimorphic switch we investigated the effects of the polyamine synthesis inhibitors CHA and DFMO. Both inhibitors showed potency and significantly reduced the dimorphic switch of *E. africanus* CBS 140360; on the other hand, CHA had high potency while DFMO had no significant effect on CBS 136260 (Fig. 6). Interestingly, while the addition of putrescine alleviated the inhibitory effect of DFMO on strain CBS 140360, spermidine supplementation resulted in an enhancement of the dimorphic transition, cementing the importance of this polyamine in the dimorphism of *E. africanus*.

To conclude, in this study, we report on the polyamine profile of *E. africanus*, with spermidine and spermine as the major polyamines, and show that the metabolism of these biogenic amines differs between strains and morphological phases. In addition, we show that spermidine, spermine, and putrescine are associated with the thermally-induced dimorphic switch from the mycelial to the pathogenic yeast-like phase—suggesting involvement in virulence. Future research should include further characterization of key enzymes in the polyamine pathways to obtain a better understanding of the synthesis of these amines. Further investigation of the involvement of polyamine metabolism in the survival and dimorphism of *E. africanus* may provide evidence on the roles of fungal polyamines in virulence. Our overall findings present initial evidence on polyamine metabolism of *E. africanus* and provide indications of their potential involvement in the pathobiology and thermal dimorphism of the fungus.

Acknowledgements

Thank you to the members of the Department of Microbiology (Stellenbosch University) for the supportive environment and helpful discussions. Thank you in particular to Prof. Eugene van Rensburg, Dr Kim Trollope, and Mr Wian Vermeulen for the valuable insights and guidance.

Author contributions

Elizaveta Koroleva (Conceptualization, Writing – original draft, Investigation, Visualization, Formal analysis), Barbra Toplis (Conceptualization, Writing – review & editing), Malcolm Taylor (Formal analysis), Corné van Deventer (Investigation), Heidi C. Steffen (Writing – review & editing), Christiaan van den Heever (Investigation), Nelesh P. Govender (Resources, Writing – review & editing), Sybren de Hoog (Writing – review & editing), and Alfred Botha (Conceptualization, Supervision, Writing – review & editing)

Supplementary data

Supplementary data are available at *FEMSYR Journal* online.

Conflict of interest: None declared

Funding

This research did not receive any specific grant from funding agencies in the public, commercial, or not-for-profit sectors.

Elizaveta Koroleva acknowledges the South African National Research Foundation for personal funding.

References

Boyce KJ, Andrianopoulos A. Fungal dimorphism: the switch from hyphae to yeast is a specialized morphogenetic adaptation allowing colonization of a host. *FEMS Microbiol Rev* 2015;**39**:797–811.

Calvo-Mendez C, Martinez-Pacheco M, Ruiz-Herrera J. Regulation of ornithine decarboxylase activity in *Mucor bacilliformis* and *Mucor rouxii*. *Exp Mycol* 1987;**11**:270–7.

Chattopadhyay MK, Tabor CW, Tabor H. Absolute requirement of spermidine for growth and cell cycle progression of fission yeast (*Schizosaccharomyces pombe*). *Proc Natl Acad Sci U S A* 2002;**99**:10330–4.

Chattopadhyay MK, Tabor CW, Tabor H. Polyamine deficiency leads to accumulation of reactive oxygen species in a *spe2*Δ mutant of *Saccharomyces cerevisiae*. *Yeast* 2006;**23**:751–61.

Cloete KJ, Valentine AJ, Stander MA *et al.* Evidence of symbiosis between the soil yeast *Cryptococcus laurentii* and a sclerophyllous medicinal shrub. *Microb Ecol* 2009;**57**:624–32.

Cogo AJD, Ferreira KDRD, Okorokov LA *et al.* Spermine modulates fungal morphogenesis and activates plasma membrane H^+-ATPase during yeast to hyphae transition. *Biol Open* 2018;**7**:1–13.

Corraliza IM, Campo ML, Soler G *et al.* Determination of arginase activity in macrophages: a micromethod. *J Immunol Methods* 1994;**174**:231–5.

Dukik K, Muñoz JF, Jiang Y *et al.* Novel taxa of thermally dimorphic systemic pathogens in the *Ajellomycetaceae* (*Onygenales*). *Mycoses* 2017;**60**:296–309.

El-Sayed ASA, George NM, Yassin MA *et al.* Purification and characterization of ornithine decarboxylase from *Aspergillus terreus*; kinetics of inhibition by various inhibitors. *Molecules* 2019;**24**:2756.

Guevara-Olvera L, Calvo-Mendez C, Ruiz-Herrera J. The role of polyamine metabolism in dimorphism of *Yarrowia lipolytica*. *J Gen Microbiol* 1993;**139**:485–93.

Han X, Shangguan J, Wang Z *et al.* Spermidine regulates mitochondrial function by enhancing eIF5A hypusination and contributes to reactive oxygen species production and ganoderic acid biosynthesis in *Ganoderma lucidum*. *Appl Environ Microb* 2022;**88**:e02037–21.

Hoving JC. *Emergomyces africanus* poses an emerging threat. *Nat Microbiol* 2024;**9**:4–5.

Hu RH, Pegg AE. Rapid induction of apoptosis by deregulated uptake of polyamine analogues. *Biochem J* 1997;**328**:307–16.

Igarashi K, Kashiwagi K. The functional role of polyamines in eukaryotic cells. *Int J Biochem Cell Biol* 2019;**107**:104–15.

Iyer RK, Kim HK, Tsoa RW *et al.* Cloning and characterization of human agmatinase. *Mol Genet Metab* 2002;**75**:209–18.

Kummasook A, Cooper CR, Sakamoto A *et al.* Spermidine is required for morphogenesis in the human pathogenic fungus, *Penicillium marneffei*. *Fungal Genet Biol* 2013;**58-59**:25–32.

Lasbury ME, Merali S, Durant PJ *et al.* Polyamine-mediated apoptosis of alveolar macrophages during *Pneumocystis* pneumonia. *J Biol Chem* 2007;**282**:11009–20.

Lerm B, Kenyon C, Schwartz IS *et al.* First report of urease activity in the novel systemic fungal pathogen *Emergomyces africanus*: a comparison with the neurotrope *Cryptococcus neoformans*. *FEMS Yeast Res* 2017;**17**:1–10.

Liu SJ, Xu JJ, Ma CL *et al.* A comparative analysis of derivatization strategies for the determination of biogenic amines in sausage and cheese by HPLC. *Food Chem* 2018;**266**:275–83.

Luqman S, Masood N, Srivastava S *et al.* A modified spectrophotometric and methodical approach to find novel inhibitors of ornithine decarboxylase enzyme: a path through the maze. *Protocol Exchange* 2013. https://doi.org/10.1038/protex.2013.045.

Mapengo RE, Maphanga TG, Grayson W *et al.* Endemic mycoses in South Africa, 2010–2020: a decade-long description of laboratory-diagnosed cases and prospects for the future. *PLOS Negl Trop Dis* 2022;**16**:e0010737.

Marshall M, Russo G, Van Etten J *et al.* Polyamines in dimorphic fungi *Curr Microbiol* 1979;**2**:187–90.

Medina HR, Morera B, Flores R *et al.* Functions of polyamines in growth and development of *Phycomyces blakesleeanus* wild-type and mutant strains. *Fungal Biol* 2022;**126**:429–37.

Miller-Fleming L, Olin-Sandoval V, Campbell K *et al.* Remaining mysteries of molecular biology: the role of polyamines in the cell. *J Mol Biol* 2015;**427**:3389–406.

Nickerson KW, Dunkle LD, Van Etten JL. Absence of spermine in filamentous fungi. *J Bacteriol* 1977;**129**:173–6.

Pfaller MA, Riley J, Gerarden T. Polyamine depletion and growth inhibition of *Cryptococcus neoformans* by α-difluoromethylornithine and cyclohexylamine. *Mycopathologia* 1990;**112**:27–32.

Preti R, Antonelli ML, Bernacchia R *et al.* Fast determination of biogenic amines in beverages by a core–shell particle column. *Food Chem* 2015;**187**:555–62.

Reddy DL, Nel J, Govender NP. Emergomycosis.*J Med Mycol* 2023;**33**:101313.

Rocha RO, Elowsky C, Pham NTT *et al.* Spermine-mediated tight sealing of the *Magnaporthe oryzae* appressorial pore–rice leaf surface interface. *Nat Microbiol* 2020;**5**:1472–80.

Rocha RO, Wilson RA. Essential, deadly, enigmatic: polyamine metabolism and roles in fungal cells. *Fung Biol Rev* 2019;**33**:47–57.

Rollins-Smith LA, Ruzzini AC, Fites JS *et al.* Metabolites involved in immune evasion by *Batrachochytrium dendrobatidis* include the polyamine spermidine. *Infect Immun* 2019;**87**:e00035–19.

San-Blas G, San-Blas F, Sorais F *et al.* Polyamines in growth and dimorphism of *Paracoccidioides brasiliensis*. *Arch Microbiol* 1997;**166**:411–3.

San-Blas G, Sorais F, San-Blas F *et al.* Ornithine decarboxylase in *Paracoccidioides brasiliensis*. *Arch Microbiol* 1996;**165**:311–6.

Schaefer K, Wagener J, Ames RM *et al.* Three related enzymes in *Candida albicans* achieve arginine- and agmatine-dependent metabolism that is essential for growth and fungal virulence. *mBio* 2020;**11**:e01845–20.

Schibalski RS, Shulha AS, Tsao BP *et al.* The role of polyamine metabolism in cellular function and physiology. *Am J Physiol Cell Physiol* 2024;**327**:C341–56.

Schwartz IS, Govender NP, Corcoran C *et al.* Clinical characteristics, diagnosis, management, and outcomes of disseminated emmonsiosis: a retrospective case series. *Clin Infect Dis* 2015;**61**:1004–12.

Schwartz IS, Lerm B, Hoving JC *et al.* *Emergomyces africanus* in soil, South Africa. *Emerg Infect Dis* 2018a;**24**:377–80.

Schwartz IS, Maphanga TG, Govender NP. *Emergomyces*: a new genus of dimorphic fungal pathogens causing disseminated disease among immunocompromised persons globally. *Curr Fung Infect Rep* 2018b;**12**:44–50.

Tang G, Xia H, Liang J *et al.* Spermidine is critical for growth, development, environmental adaptation, and virulence in *Fusarium graminearum*. *Front Microbiol* 2021;**12**:765398.

Toplis B, Bosch C, Schwartz IS *et al.* The virulence factor urease and its unexplored role in the metabolism of *Cryptococcus neoformans*. *FEMS Yeast Res* 2020;**20**:1–14.

Toplis B, Bosch C, Stander M *et al.* A link between urease and polyamine metabolism in *Cryptococcus neoformans*. *Microb Pathog* 2021;**158**:1–7.

Valdés-Santiago L, Guzmán-De-Peña D, Ruiz-Herrera J. Life without putrescine: disruption of the gene-encoding polyamine oxidase in *Ustilago maydis odc* mutants. *FEMS Yeast Res* 2010;**10**:928–40.

Valdés-Santiago L, Ruiz-Herrera J. Stress and polyamine metabolism in fungi. *Front Chem* 2014;**1**:1–10.

Vindu A, Shin BS, Choi K *et al.* Translational autoregulation of the *S. cerevisiae* high-affinity polyamine transporter Hol1. *Mol Cell* 2021;**81**:1–15.

Walters DR, Cowley T. Formation of cadaverine derivatives in *Saccharomyces cerevisiae*. *FEMS Microbiol Lett* 1996;**145**:255–9.

Zarb J, Walters DR. The formation of cadaverine, aminopropylcadaverine and N,N bis (3aminopropyl) cadaverine in mycorrhizal and phytopathogenic fungi. *Lett Appl Microbiol* 1994;**19**:277–80.

Zhang AX, Mouhoumed AZ, Tong SM *et al.* BrlA and AbaA govern virulence-required dimorphic switch, conidiation, and pathogenicity in a fungal insect pathogen. *mSystems* 2019;**4**:e00140–19.

Received 17 July 2024; **revised** 4 November 2024; **accepted** 28 November 2024